Chemical Engineering Journal 483 (2024) 149388

Contents lists available at ScienceDirect

Chemical Engineering Journal

journal homepage: www.elsevier.com/locate/cej

Stretchable and biodegradable composite films for disposable, antibacterial, radiative cooling system

Won Bae Han [a,b,c,1], Heeseok Kang [a,d,1], Se-Yeon Heo [e,1], Yelynn Ryu [f], Gyuil Kim [g], Gwan-Jin Ko [a], Jeong-Woong Shin [a], Tae-Min Jang [a], Sungkeun Han [a], Jun Hyeon Lim [a], Chan-Hwi Eom [a], Young Min Song [e,*], Suk-Won Hwang [a,h,i,*]

[a] KU-KIST Graduate School of Converging Science and Technology, Korea University, 145 Anam-ro, Seongbuk-gu, Seoul 02841, Republic of Korea
[b] IEN Center for Wearable Intelligent Systems and Healthcare, Georgia Institute of Technology, Atlanta, GA 30332, USA
[c] George W. Woodruff School of Mechanical Engineering, Georgia Institute of Technology, Atlanta, GA 30332, USA
[d] Center for Advanced Biomolecular Recognition, Biomedical Research Institute, Korea Institute of Science and Technology (KIST), 5 Hwarang-ro 14-gil, Seongbuk-gu, Seoul 02792, Republic of Korea
[e] School of Electrical Engineering and Computer Science, Gwangju Institute of Science and Technology (GIST), 123 Cheongdangwagi-ro, Buk-gu, Gwangju 61005, Republic of Korea
[f] Department of Architecture, Korea University, 145 Anam-ro, Seongbuk-gu, Seoul 02841, Republic of Korea
[g] School of Biomedical Engineering, Korea University, 145 Anam-ro, Seongbuk-gu, Seoul 02841, Republic of Korea
[h] Department of Integrative Energy Engineering, Korea University, 145 Anam-ro, Seongbuk-gu, Seoul 02841, Republic of Korea
[i] Center for Biomaterials, Biomedical Research Institute, Korea Institute of Science and Technology (KIST), 5 Hwarang-ro 14-gil, Seongbuk-gu, Seoul 02792, Republic of Korea

ARTICLE INFO

Keywords:
Biodegradability
Polymer composites
Magnesium oxides
Radiative cooling
Antibacterial effect

ABSTRACT

Materials that inhibit bacteria and viruses, while ensuring thermal comfort and physical ease, can play a significant role in the realm of protective textiles and equipment for outdoor healthcare activities, particularly in the context of recent global pandemics. Here, we develop radiative cooling and antibacterial composites consisting of stretchable, biodegradable poly(lactide-co-ε-caprolactone) (PLCL) and magnesium oxide (MgO) particles via a scalable solution casting process. Precise control over the size and composition of the particles within the polymer matrix through theoretical and experimental analyses achieves sub-ambient daytime radiative cooling (△T, ~7℃) under diverse weather conditions. Bactericidal MgO particles through surface treatments realize a remarkable reduction of bacterial cell viability by ~100 % in 8 h. The overall results suggest that materials with thermal and infection control capability as well as disposable characteristics have the potential to reduce plastic waste beyond the spread of infection.

1. Introduction

Daytime radiative cooling – a passive cooling technology that allows objects to cool below the ambient air temperature by reflecting sunlight and radiating heat into the cold outer space – has received significant attention due to sustainable and zero-energy operation. Such technology has been applied to research areas involving personal thermal management [1–3], reduced air-conditioning energy consumption in residential/industrial areas [4–6], energy generation [7–9], and water harvesting/purification [10–12]. Since strong solar reflectance and emissivity in the atmosphere's long-wave infrared (LWIR) region are key factors to achieve the efficient cooling property, many researchers have explored various material types and structural designs including multilayered films [13–15], metamaterials [16–18], porous and fibrous polymer membranes [19–22], and inorganic–organic hybrid composites [23–26]. The last stood out for superior cooling efficacy through intrinsic infrared absorption of chemical bonds of polymer matrices and effective solar scattering of inorganic particles with carefully controlled

* Corresponding authors at: School of Electrical Engineering and Computer Science, Gwangju Institute of Science and Technology (GIST), 123 Cheongdangwagi-ro, Buk-gu, Gwangju 61005, Republic of Korea (Y.M. Song); KU-KIST Graduate School of Converging Science and Technology, Korea University, 145 Anam-ro, Seongbuk-gu, Seoul 02841, Republic of Korea (S.-W. Hwang).
E-mail addresses: ymsong@gist.ac.kr (Y.M. Song), dupong76@korea.ac.kr (S.-W. Hwang).
[1] Won Bae Han, Heeseok Kang, and Se-Yeon Heo contributed equally to this work.

https://doi.org/10.1016/j.cej.2024.149388
Received 9 December 2023; Received in revised form 31 January 2024; Accepted 3 February 2024
Available online 5 February 2024

sizes [3,27], and inherent physical/electrical functions of the particles offer the opportunity to broaden the application [26,28,29].

The recent global pandemic greatly amplified interest or demand in antibacterial materials that are essential for maintaining healthy and sanitary environments, particularly in the field of protective equipment (bodysuit, gloves, and shoes) for medical staffs engaged in disease surveillance and quarantine activities. Metal oxide particles (e.g., copper oxide (CuO), silver oxide (Ag_2O), and titanium oxide (TiO_2)) have been developed to address such concerns through collective antibacterial mechanisms including reactive oxygen species, photocatalyst, direct physical damage, released metal ions, and alkaline effect [30–33], although there are few reported examples of forms combined with additional functions other than antibacterial function.

Here, we propose a stretchable and biodegradable composite that

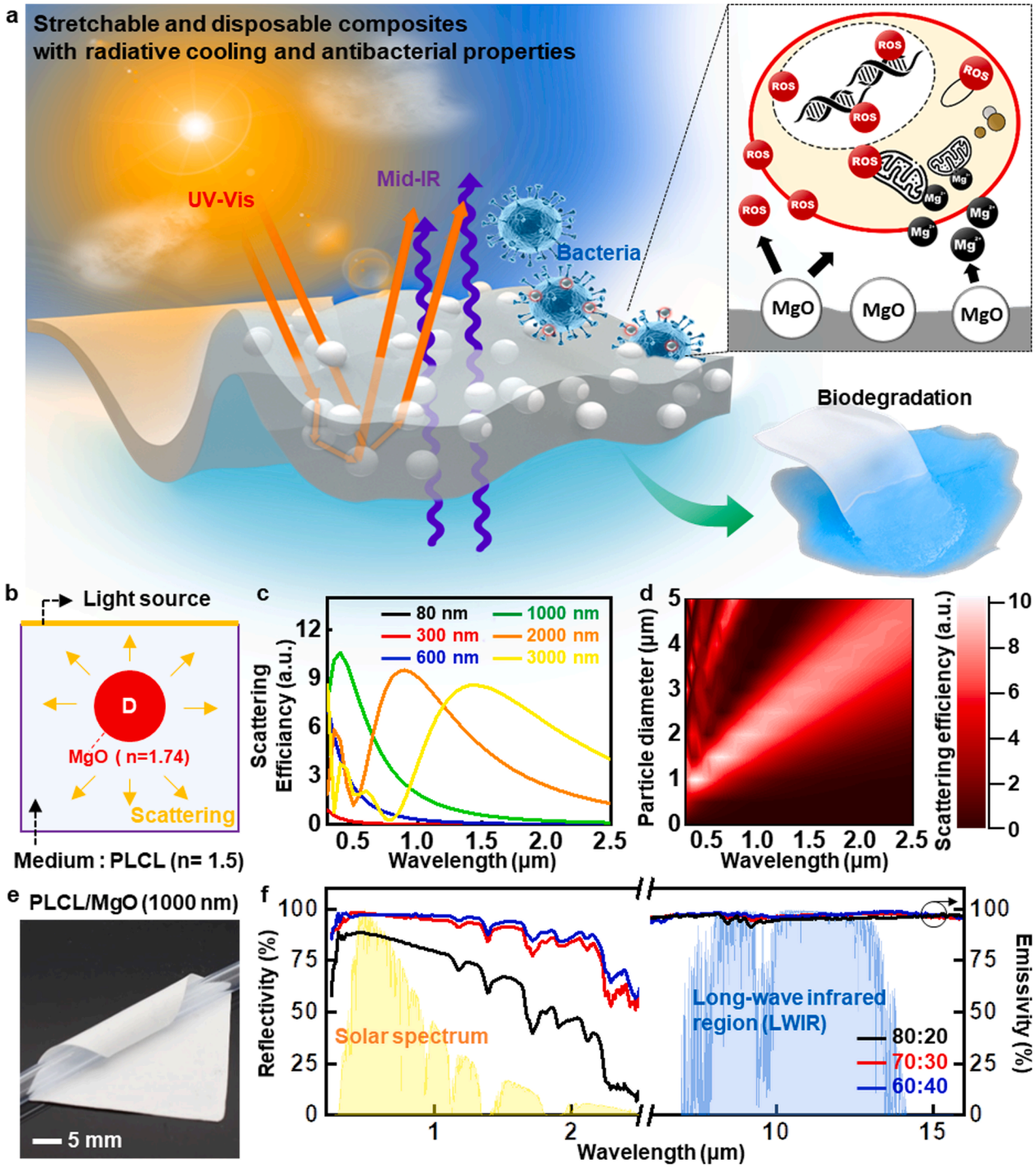

Fig. 1. Stretchable and disposable composites with radiative cooling and antibacterial properties. (a) Schematic illustration of a stretchable, biodegradable, and antibacterial radiative cooler film based on poly(lactide-co-ε-caprolactone) (PLCL) and magnesium oxide (MgO) particles, with the bactericidal mechanism in the inset. (b) Two-dimensional Finite-difference time-domain (FDTD) simulation of a PLCL matrix embedded with MgO particles for solar reflectance. (c) Calculated scattering efficiencies of PLCL/MgO films with different particle diameters (80, 300, 600, 1000, 2000, and 3000 nm). (d) Scattering efficiency of PLCL/MgO film in the range of particle diameter from 0 to 5 μm. (e) Optical image of a thin composite film containing MgO particles with a diameter of 1000 nm. (f) Spectral UV–visible–infrared reflectivity/emissivity of PLCL/MgO films with volume ratios of 80:20, 70:30, and 60:40 (PLCL:MgO).

contains the particular features of radiative cooling and antibacterial properties, based on PLCL elastomer and MgO particles, which stand out for their high solar scattering and bactericidal effects among various biodegradable metal oxides (Previous works on biodegradable metal oxide particles for radiative cooling and antibacterial activity are summarized in Table S1). Through a combination of theoretical simulation and experimental analysis, we optimize the size and concentration of MgO particles within the polymer matrix to strike a balance between the optical requirements for effective radiative cooling and the essential mechanical resilience. Evaluations on outdoor cooling performance, coupled with a practical demonstration of cooling gloves, confirm the sub-ambient daytime radiative cooling capable of a substantial temperature reduction of ~ 7 °C. Antibacterial tests using Escherichia coli (E. coli) validate outstanding bactericidal activity of surface-modified composites, that can eliminate 100 % bacterial cell within 8 h. The successful integration of these comprehensive attributes, including stretchability, biodegradability, radiative cooling, and antibacterial activity, in a single composite marks a significant milestone in materials science with potential implications for diverse applications requiring hygiene as well as thermal comfort and disposability.

2. Results and discussion

2.1. Stretchable, biodegradable, antibacterial, radiative cooling composites

Fig. 1a illustrates a stretchable, antibacterial radiative cooling system that comprised of dissolvable magnesium oxide (MgO) particles embedded in an elastic, degradable poly(lactide-co-ε-caprolactone) (PLCL) matrix. This elastomeric polymer exhibited excellent emission property of heat owing to abundant chemical bonds with vibration modes in the long-wave infrared region (LWIR; wavelength (λ) 4 to 16 μm) [9]. The dispersed MgO particles within the polymer matrix were effective not only in scattering the solar spectrum (λ, ~0.3 to 2.5 μm) (Fig. S1), but also in antibacterial activity through several mechanisms involving released magnesium ions, reactive oxygen species, and alkaline effect, as studied in previous literatures [34–37]. Fig. 1b–d presents theoretical results of the two-dimensional finite-difference time-domain (FDTD) method designed to explore the optical effects of MgO particles within PLCL. Since particle sizes significantly influence the range of scattering wavelength [3,27], we evaluated particles with various diameters (80, 300, 600, 1000, 2000, and 3000 nm) for solar reflectance using Mie scattering theory. The results revealed that scattering peaks exhibited a redshift as the particle diameter increased, and the highest scattering efficiency was achieved by 1000 nm particles in diameter, as

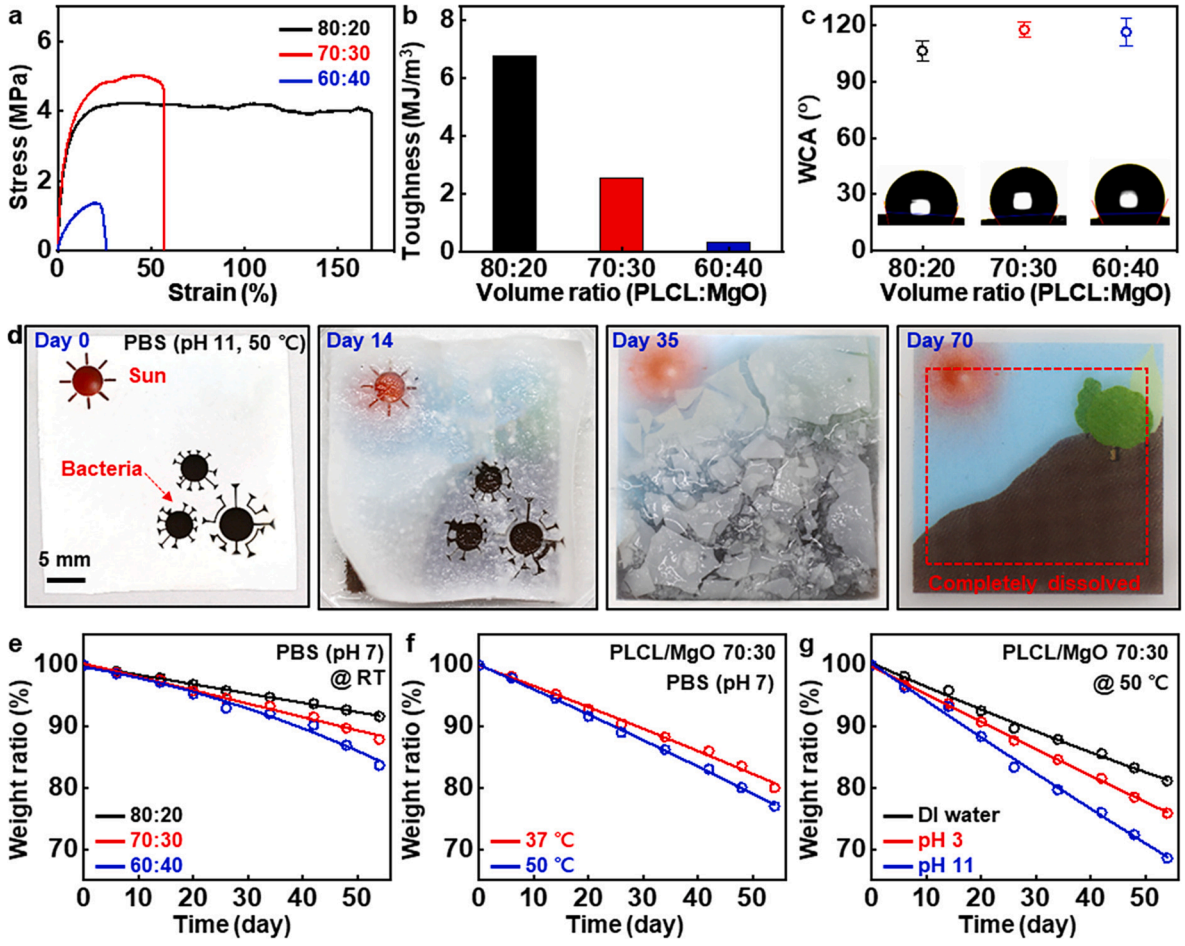

Fig. 2. Mechanical, physical, and biochemical properties of PLCL/MgO films. (a) Stress–strain curves of PLCL/MgO films with different ratios of the embedded particles (black, 80:20; red, 70:30; blue, 60:40). (b,c) Effects of MgO concentrations on toughness (b) and water contact angle (WCA) (c) of PLCL/MgO mixtures. (d) Collection of temporal dissolution images of a thin PLCL/MgO sheet with a cartoon under accelerated condition (phosphate-buffered saline (PBS), pH 11, at 50 °C), after day 0 (left), day 14 (middle left), day 35 (middle right), and day 70 (right). (e) Time-dependent changes in weight ratios of PLCL/MgO membranes with different ratios of PLCL to MgO in PBS (pH 7) at room temperature. (f,g) Effects of temperature (f) and pH (g) on dissolution rates of PLCL/MgO films in PBS. (For interpretation of the references to color in this figure legend, the reader is referred to the web version of this article.)

confirmed by measured optical spectra in Fig. S2. The white color of a PLCL/MgO film with 1000 nm diameter particles also validated the high solar reflectance (Fig. 1e and Fig. S3). The concentration of the particles was closely correlated with the solar reflectivity since light scattering occurred at PLCL/MgO interfaces (Fig. 1f). As a result, PLCLs blended with relatively large amounts of the filler (70:30 and 60:40) yielded high solar reflectivity that can compete with state-of-the-art radiative cooling materials [38,39]. Moreover, such optical performance remained unchanged even under strains up to 40 % (Fig. S4). Fabrication cost and density of PLCL/MgO composites are presented in Table S2.

2.2. Mechanical, physical, and biochemical properties of PLCL/MgO films

Fig. 2a presents stress–strain curves of PLCL/MgO films with different volume ratios of PLCL to MgO. As the MgO fraction increased from 20 % to 30 %, the elastic modulus somewhat increased, while the elongation at break reduced from ~ 170 % to ~ 60 %. When MgO particles were incorporated at 40 %, both modulus and maximum strain dramatically decreased, presumably due to insufficient binding forces between particles [40]. Such tendency was also evident in the result of the toughness, calculated by integrating the area under the stress–strain curve. (Fig. 2b). The polymeric composite with the ratio 80:20 exhibited the highest value of ~ 7 MJ/m^3, which was 20-fold higher than that of the film with the ratio 60:40. Fig. 2c shows water contact angles (WCAs) of PLCL/MgO films. The addition of particles roughened the film surface, resulting in increased WCAs from 100° (pristine PLCL film [41]) to 105 ~ 120°, practically applicable for a self-cleaning system [42]. Fig. 2d displays sequential degradation images of PLCL/MgO films (thickness, 100 μm) during immersion in phosphate buffered saline (PBS; pH 11) at 50 °C as an accelerated condition. The film gradually dissolved via hydrolysis of MgO particles ($MgO + H_2O \leftrightarrow Mg(OH)_2$ [43]) and the ester bonds of PLCL[44], completely disappearing 70 days after immersion. The dissolution rate of the PLCL/MgO films varied depending on MgO fractions. High MgO fractions facilitated water diffusion through polymer-particle interfaces, leading to enhanced hydrolytic reactions and a fast degradation rate. Similar trend was observed in measurements of water vapor transmission rate (WVTR) (Fig. S5). Changes in temperature and pH level affected the dissolution behavior. Increase in temperature accelerated chemical reactions, resulting in the rapid dissolution of PLCL/MgO films (Fig. 2f), and the degradation rate was also faster in acidic (pH 3) and basic (pH 11) solutions than the one in deionized (DI) water, consistent with previous reports [44,45].

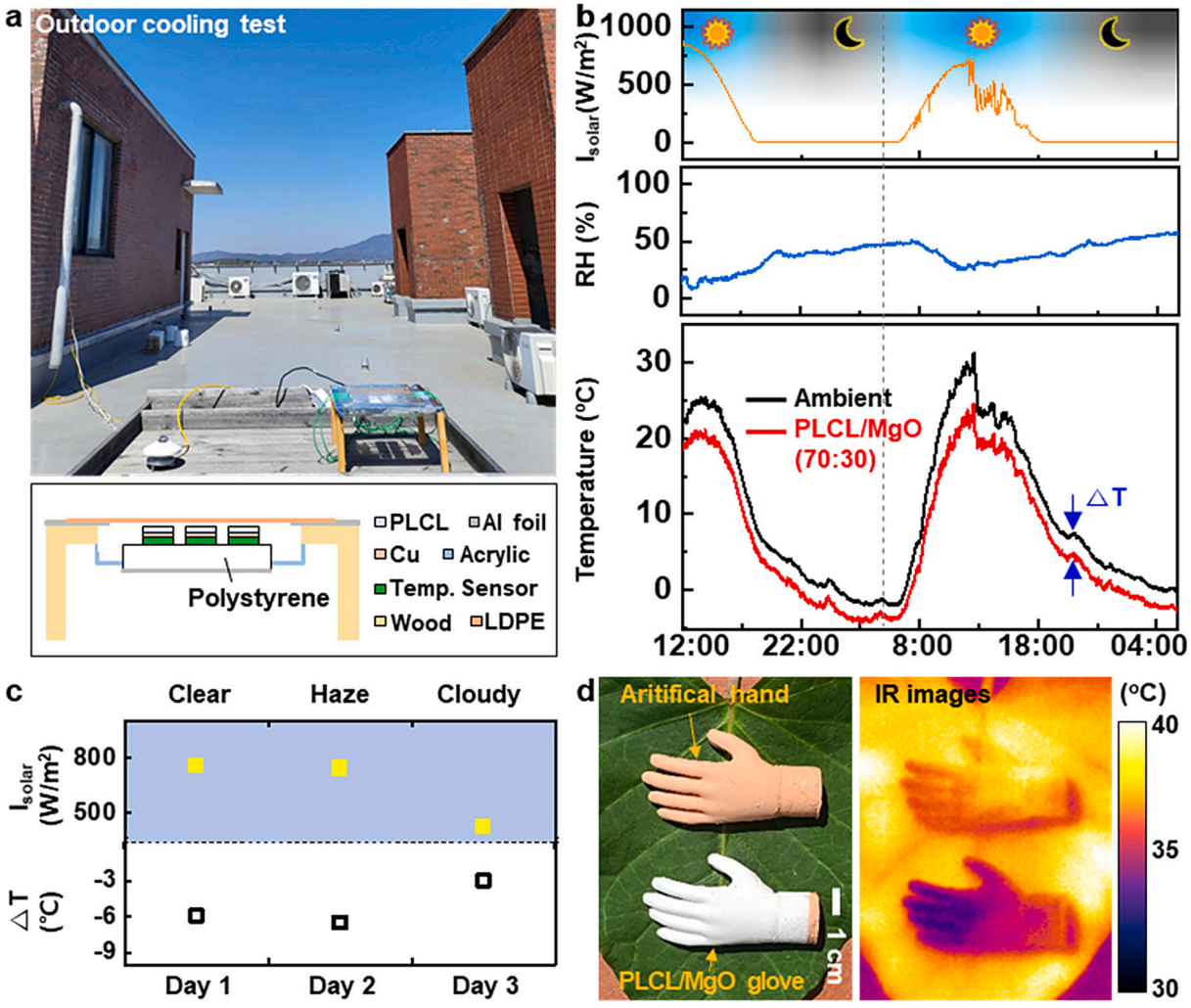

Fig. 3. Sub-ambient daytime cooling performance of PLCL/MgO composite. (a) Photograph of the overall experiment setup (top) and schematic configuration of a radiative cooling system (bottom), for evaluation on the outdoor cooling performance of PLCL/MgO composites under sunlight. (b) Real-time measurements of solar irradiance, relative humidity, and temperature of PLCL/MgO films (70:30) over ~ 2 days. (c) Average solar intensity and cooling temperature (△T) of the PLCL/MgO films under various weather conditions. (d) Optical image (left) and corresponding infrared (IR) thermogram (right) of an artificial hand without (top) and with (bottom) wearing PLCL/MgO-based gloves.

2.3. Daytime radiative cooling performance of PLCL/MgO composite

To assess the radiative cooling performance of PLCL/MgO composites, we measured a tendency of ambient and PLCL/MgO temperatures in a custom-made chamber with a convection shield on an outdoor rooftop at Gwangju Institute of Science and Technology (GIST; 35°13′36.5″N, 126°50′24.0″E) for ~ 2 days (Fig. 3a). Real-time, continuous recordings revealed that the use of PLCL/MgO films consistently achieved sub-ambient cooling with a maximum temperature reduction (△T) of ~ 7 ℃ under diverse sky conditions and humidity levels (Fig. 3b). Such cooling performance was maintained even under hazy and cloudy conditions, which typically impeded radiative heat emission into the cold universe [46,47], resulting in △T values of ~ 6 ℃ and ~ 3 ℃ in daytime, respectively (Fig. 3c and Fig. S6). This cooling property could be attributed to the high solar reflectance (~98 % at 500 nm wavelength) and excellent LWIR emissivity (~97 %). Given the cooling capability and mechanical resilience, the PLCL/MgO film can be used in a wide range of applications, particularaly in the realm of disposable textiles for outdoor activities. As an example, Fig. 3d presents biodegradable PLCL/MgO composites-based gloves with a cooling effect. Artificial hands with or without the glove were placed under intense sunlight, and infrared (IR) thermography showed that the glove lowered the temperature by ~ 8 ℃ when compared to the bare hand, which confirmed the practical performance. Evaluation on wearability and cooling effect of a PLCL/MgO composite-based glove on the human body appear in Fig. S7.

2.4. Antibacterial property of PLCL/MgO composite

The antibacterial properties of the disposable coolant material are useful in minimizing the transmission of infections under healthcare environments. Fig. 4a illustrates an approach to enhancement of the antibacterial effect through exposure of MgO particles that is well-known for antibacterial activity [37]. Briefly, we removed polymeric components to expose MgO particles on the film surface via reactive ion etching (RIE), and then improved hydrophobicity of the resulting film with a self-assembled monolayer (SAM) treatment for impeding microbial adhesion. Scanning electron microscopy (SEM) images and

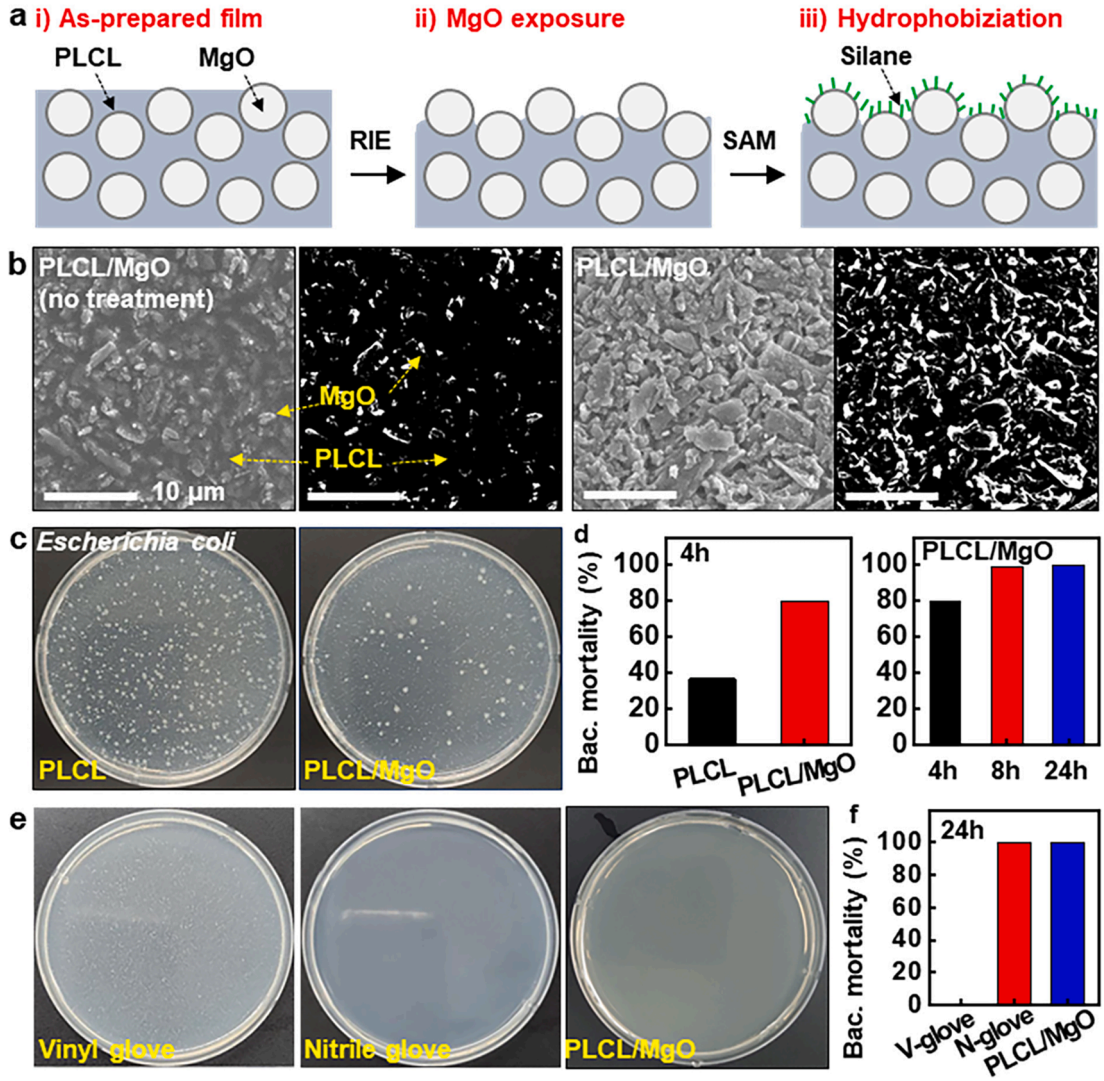

Fig. 4. Antibacterial property of PLCL/MgO composite. (a) Schematic drawing of a fabrication process of a highly effective bactericidal film: 1) neat PLCL/MgO film preparation, 2) MgO exposure by reactive ion etching (RIE), and 3) hydrophobization by silane treatment. (b) Scanning electron microscopy (SEM) images of PLCL/MgO without and with surface treatments, along with binary images processed by ImageJ software to estimate the exposed area of MgO particles. (c) Images of the colonies of *Escherichia coli* cultured on PLCL and PLCL/MgO films for 4 h. (d) Comparison of mortality rates of *E. coli* on PLCL and surface-treated PLCL/MgO films (left), and time-dependent changes in the bactericidal effect of surface-treated PLCL/MgO films (right). (e,f) Photographs (e) and corresponding bacterial mortality (f) of *E. coli* cultured on a vinyl glove, a nitrile glove, and surface-treated PLCL/MgO film for 24 h.

corresponding binary images processed by ImageJ software in Fig. 4b revealed that the engineered PLCL/MgO films exhibited larger MgO surface area compared to that of the pristine film. The hydrophobic nature of the PLCL/MgO film was confirmed by water contact angle analysis in Fig. S8. Here, it is noteworthy that the surface treatments had a negligible impact on the spectral performance of PLCL/MgO films (Fig. S9). Fig. 4c displays the antibacterial performance of the PLCL/MgO films against gram-negative bacteria, *Escherichia coli* (*E. coli*). The films validated excellent antibacterial efficiency after 4 h of incubation, leading to a significant reduction in the number of live bacterial cells, whereas a large amount of bacteria survived on the pristine PLCL films. The bacterial mortality rate (left, Fig. 4d) reached ~ 40 % and ~ 80 % for the pristine PLCL (black) and PLCL/MgO (red) films, and prolonged incubation times (right, Fig. 4d) further increased the bacterial mortality of the PLCL/MgO films, eventually reaching non-measurable levels of viable bacteria after 8 h of incubation. Fig. 4e provided antibacterial activities between the PLCL/MgO films and commercial products, i.e., vinyl and nitrile gloves, when exposed to *E. coli* over 24 h. The vinyl gloves were not effective in inhibition of bacterial growth, while both the nitrile gloves and PLCL/MgO films showed strong bactericidal activity (mortality, ~100 %). The overall result, coupled with its biocompatibility [44,48–50], highlights the potential applicability of the PLCL/MgO composite as protective textiles with thermal comfort as well as hygiene.

3. Conclusion

The concepts, materials, and fabrication method proposed here present a practical approach to fabricate a stretchable, disposable hybrid composite with radiative cooling and antibacterial capabilities. Incorporation of MgO particles with the theoretically optimized dimension into the elastic PLCL polymer effectively scattered sunlight while retaining excellent LWIR emissivity, achieving sub-ambient daytime radiative cooling (~7 ℃) even under unfavorable weather conditions. Surface modification of the composite demonstrated a remarkable antibacterial property, which the viability of cells was reduced to ~ 0 % after an 8-hour incubation period. Overall, such properties coupled with mechanical resilience and biodegradability, offer invaluable potential for a wide range of applications, particularly in sustainable and disposable textiles where both thermal comfort and hygiene are critical.

4. Experimental section

Finite-difference time-domain (FDTD) simulations: FDTD simulations, using the FullWAVE Solutions software from Rsoft (RSoft Design Group, Synopsys, USA), were conducted to assess the impact of MgO (magnesium oxide) particles on the optical properties of poly(L-lactide-co-ε-caprolactone) (PLCL). Due to limitations in computational resources, two-dimensional models were employed, and the results closely matched those from three-dimensional models, considering transverse magnetic (TM) oscillation with respect to particle radius. Scattering cross-sections of circular MgO particles of various sizes within a PLCL matrix were obtained for solar wavelengths ranging from 0.3 to 2.5 μm, assuming constant refractive indices of 1.5 for PLCL and 1.74 for MgO particles.

Preparation of PLCL/MgO hybrid composite films: Details in synthesis of PLCL was described in our previous report [44]. PLCL solution was prepared by dissolving PLCL in dimethylformamide (DMF) at a concentration of 10 % (w/v) and mixed overnight. MgO nanoparticles with various diameters (300 nm, 600 nm, 1000 nm, 2000 nm) were added into the PLCL solution to achieve volume ratios (PLCL:MgO) of 80:20, 70:30, and 60:40, and stirred vigorously for 3 h. Then, the mixed solutions were poured into polydimethylsulfoxide (PDMS) molds. After solvent evaporation at 50 °C for 24 h, the dried films (thickness, ~500 μm) were achieved by gentle detachment from the mold. Here, the high viscosity of the PLCL/MgO solution played a crucial role in preventing settling of MgO particles during the drying process and thus ensuring a uniform distribution of particles within the polymer matrix (Cross-sectional SEM image of PLCL/MgO (70:30) film appears in Fig. S10). To enhance antibacterial effect, MgO particles within PLCL matrix were exposed by the following surface treatments. The surface of composite film was etched by reactive ion etching system (RIE, JVRIE17-8TM, JVAC, South Korea) under O_2 and CF_4 atmosphere (rate, 20 sccm) at an operating power of 200 W for 10 min. Higher tolerance of metal oxide to etching compared to polymer resulted in effective elimination of polymeric components and revealing of MgO particles (antibacterial agents) on the film surface. For preventing microbial adhesion, the film was then placed in a vacuum chamber with 100 μL of trichloro(1H, 1H, 2H, 2H-perfluorooctyl)silane (Sigma-Aldrich, South Korea), and vapor phase deposition of self-assembled silane monolayer was carried out for 2 h.

Spectral characterization: Optical absorption properties of PLCL/MgO composites were examined in a spectral range from 280 nm to 2500 nm using an ultraviolet–visible-near-infrared spectrometer (Lambda 950, Perkin Elmer, Inc., USA) and in the long-wave infrared region (4 μm to 16 μm) using a Fourier-transform infrared spectrometer (VERTEX 70v, Bruker, USA) equipped with a gold-coated integrating sphere. The emissivity was determined by subtracting the sum of reflectivity and transmittance values from 100.

Characterization of mechanical and physical properties: For mechanical property measurements, PLCL/MgO composite films with various volume ratios (80:20, 70:30, and 60:40) were cut into a dumbbell shape (ASTM D638), and these specimens were subjected to mechanical tensile tests at a constant stretching rate of 6 mm/min using a universal mechanical testing system (Instron 5900 series, Instron, USA). Toughness was calculated by integrating the area under the obtained stress–strain curves. Water contact angle (WCA) was measured by dropping deionized (DI) water of ~ 6 μL of on each PLCL/MgO composite film under ambient conditions, using a contact angle meter (Phoenix-MT(M), SEO, South Korea). Water vapor transmission rate (WVTR) was measured by ASTM E96 standards with minor modifications. Vials of 30 mL with an opening diameter of 17 mm were filled with 20 mL of deionized (DI) water and securely sealed with PLCL/MgO composite films using an epoxy. These vials were placed in a chamber at a temperature of 35 °C and ~ 30 % ± 10 % relative humidity. Periodic measurements of the vials' weight loss, attributable to water evaporation, were taken and divided by the opening area to calculate the WVTR.

Biodegradation test: PLCL/MgO composite samples were immersed in PBS (pH 7) at room temperature for ~ 50 days. Each sample was removed every week, rinsed with DI water, and dried in a freeze dryer (TFD 8503, IlShinBioBase, South Korea). The weight ratio was calculated using the formula, weight ratio (%) = W_a / W_b x 100, where W_b and W_a are the weights of the samples before and after the immersion, respectively. Additionally, we evaluated the effects of temperature and pH on the dissolution rate of composites by immersing PLCL/MgO composite sample with a volume ratio of 70:30 in PBS (pH 7) at temperatures of 37 °C and 50 °C and in DI water or PBS with different pH levels of 3 and 11 for ~ 50 days.

Outdoor cooling measurements: Outdoor cooling performance assessments of PLCL/MgO composites were conducted using a custom-made chamber with a convection shield on an outdoor rooftop at Gwangju Institute of Science and Technology (GIST; 35°13′36.5″N, 126°50′24.0″E) from 03/24/23 to 03/30/23. Adhesive temperature sensors (ST-50; RKC Instrument Inc., Japan) electrically connected to a data logger (RDXL6SD; Omega Engineering, USA) were attached on the back surface of PLCL/MgO composites. The samples were placed on a polystyrene block within the custom-made chamber to minimize heat interference. To mitigate potential ambient air heating due to solar irradiation, an ambient air sensor (model RTD-805, Omega Engineering, USA) was housed in an aluminum box with pores for air flowing. Next to this experimental setup, a pyranometer (model CMP; Kipp & Zonen, Netherlands) was placed to monitor both direct and scattered solar

radiation.

Fabrication of PLCL/MgO cooling gloves: Artificial hand was fabricated by pouring Ecoflex 00–50 (1A:1B) mixed with a little amount of yellow dye into an ultraviolet (UV) sensitive resin-based mold constructed by a 3D printer (Photon mono x 6 k, Anycubic, China) and curing at ambient temperature for 4 h. The resulting artificial hand was then immersed in a PLCL/MgO (70:30) solution, followed by drying in oven at 80 ℃ for 3 h. This coating process was repeated to obtain ~ 500 μm-thick gloves.

Antibacterial test: The antibacterial efficacy of PLCL/MgO composite was assessed against *Escherichia coli* (*E. coli*). Initially, 0.4 mL of *E. coli* suspension, pre-adjusted with liquid nutrient broth to achieve a concentration of 6 x 10^5 CFU/mL, was dispensed onto a composite surface (50 mm x 50 mm) in a petri dish and the sample was covered with a polypropylene film (40 mm x 40 mm). After incubating at 35 ± 1 ℃ with a relative humidity exceeding 90 % for predetermined durations (4, 8, and 24 h), the sample was gently rinsed with soya casein digest lecithin polysorbate (SCDLP) broth to remove non-adhered cells, and the cell was collected through vortexing. Finally, 1 mL of the cell suspension was spread on a nutrient agar plate and incubated at 35 ± 1 ℃ for 48 h, followed by counting the number of viable cells on the film.

Data availability.

The data that support the findings of this study are available from the corresponding author upon reasonable request.

CRediT authorship contribution statement

Won Bae Han: Conceptualization, Data curation, Investigation, Methodology, Visualization, Writing – original draft, Writing – review & editing. **Heeseok Kang:** Writing – original draft, Methodology, Investigation, Formal analysis, Data curation, Conceptualization. **Se-Yeon Heo:** Writing – original draft, Methodology, Investigation, Formal analysis, Data curation, Conceptualization. **Yelynn Ryu:** Visualization, Methodology, Investigation. **Gyuil Kim:** Methodology, Investigation. **Gwan-Jin Ko:** Methodology, Investigation. **Jeong-Woong Shin:** Methodology, Investigation. **Tae-Min Jang:** Methodology, Investigation. **Sungkeun Han:** Methodology, Investigation. **Jun Hyeon Lim:** Investigation, Methodology. **Chan-Hwi Eom:** Investigation. **Young Min Song:** Conceptualization, Supervision, Writing – original draft, Writing – review & editing. **Suk-Won Hwang:** Writing – review & editing, Writing – original draft, Supervision, Conceptualization.

Declaration of competing interest

The authors declare that they have no known competing financial interests or personal relationships that could have appeared to influence the work reported in this paper.

Data availability

Data will be made available on request.

Acknowledgements

This work was supported by the Korea Institute of Science and Technology (KIST) Institutional Program (2E32501-23-106), the National Research Foundation of Korea (NRF) grant funded by the Korea government (the Ministry of Science and ICT, MSIT) (RS-2022-00165524, NRF-2022M3H4A1A02085336, NRF-2022M3C1A3081312), the development of technologies for electroceuticals of National Research Foundation (NRF) funded by the Korean government (MSIT) (RS-2023-00220534), ICT Creative Consilience program through the Institute of Information & Communications Technology Planning & Evaluation(IITP) grant funded by the Korea government (MSIT) (IITP-2024-2020-0-01819), and Start up Pioneering in Research and Innovation (SPRINT) through the Commercialization Promotion Agency for R&D Outcomes (COMPA) grant funded by the Korea government (Ministry of Science and ICT) (1711198921).

Appendix A. Supplementary data

Supplementary data to this article can be found online at https://doi.org/10.1016/j.cej.2024.149388.

References

[1] P.-C. Hsu, A.Y. Song, P.B. Catrysse, C. Liu, Y. Peng, J. Xie, S. Fan, Y. Cui, Radiative human body cooling by nanoporous polyethylene textile, Sci. 353 (2016) 1019–1023.
[2] P.-C. Hsu, C. Liu, A.Y. Song, Z. Zhang, Y. Peng, J. Xie, K. Liu, C.-L. Wu, P. B. Catrysse, L. Cai, S. Zhai, A. Majumdar, S. Fan, Y. Cui, A dual-mode textile for human body radiative heating and cooling, Sci. Adv. 3 (2017) e1700895.
[3] S. Zeng, S. Pian, M. Su, Z. Wang, M. Wu, X. Liu, M. Chen, Y. Xiang, J. Wu, M. Zhang, Q. Cen, Y. Tang, X. Zhou, Z. Huang, R. Wang, A. Tunuhe, X. Sun, Z. Xia, M. Tian, M. Chen, X. Ma, L. Yang, J. Zhou, H. Zhou, Q. Yang, X. Li, Y. Ma, G. Tao, Hierarchical-morphology metafabric for scalable passive daytime radiative cooling, Sci. 373 (2021) 692–696.
[4] J. Mandal, Y. Fu, A.C. Overvig, M. Jia, K. Sun, N.N. Shi, H. Zhou, X. Xiao, N. Yu, Y. Yang, Hierarchically porous polymer coatings for highly efficient passive daytime radiative cooling, Science 362 (2018) 315–319.
[5] T. Li, Y. Zhai, S. He, W. Gan, Z. Wei, M. Heidarinejad, D. Dalgo, R. Mi, X. Zhao, J. Song, J. Dai, C. Chen, A. Aili, A. Vellore, A. Martini, R. Yang, J. Srebric, X. Yin, L. Hu, A radiative cooling structural material, Sci. 364 (2019) 760–763.
[6] S. Wang, T. Jiang, Y. Meng, R. Yang, G. Tan, Y. Long, Scalable thermochromic smart windows with passive radiative cooling regulation, Sci. 374 (2021) 1501–1504.
[7] A.P. Raman, W. Li, S. Fan, Generating light from darkness, Joule. 3 (2019) 2679–2686.
[8] W. Ren, Y. Sun, D. Zhao, A. Aili, S. Zhang, C. Shi, J. Zhang, H. Geng, J. Zhang, L. Zhang, J. Xiao, R. Yang, High-performance wearable thermoelectric generator with self-healing, recycling, and Lego-like reconfiguring capabilities, Sci. Adv. 7 (2021) eabe0586.
[9] W.B. Han, S.-Y. Heo, D. Kim, S.M. Yang, G.-J. Ko, G.J. Lee, D.-J. Kim, K. Rajaram, J. H. Lee, J.-W. Shin, T.-M. Jang, S. Han, H. Kang, J.H. Lim, D.H. Kim, S.H. Kim, Y. M. Song, S.-W. Hwang, Zebra-inspired stretchable, biodegradable radiation modulator for all-day sustainable energy harvesters, Sci. Adv. 9 (2023) eadf5883.
[10] H. Kim, S.R. Rao, E.A. Kapustin, L. Zhao, S. Yang, O.M. Yaghi, E.N. Wang, Adsorption-based atmospheric water harvesting device for arid climates, Nat. Commun. 9 (2018) 1191.
[11] I. Haechler, H. Park, G. Schnoering, T. Gulich, M. Rohner, A. Tripathy, A. Milionis, T.M. Schutzius, D. Poulikakos, Exploiting radiative cooling for uninterrupted 24-hour water harvesting from the atmosphere, Sci. Adv. 7 (2021) eabf3978.
[12] X. Huang, J. Mandal, J. Xu, A.P. Raman, Passive freezing desalination driven by radiative cooling, Joule. 6 (2022) 2762–2775.
[13] A.P. Raman, M.A. Anoma, L. Zhu, E. Rephaeli, S. Fan, Passive radiative cooling below ambient air temperature under direct sunlight, Nat. 515 (2014) 540–544.
[14] L. Zhou, H. Song, J. Liang, M. Singer, M. Zhou, E. Stegenburgs, N. Zhang, C. Xu, T. Ng, Z. Yu, B. Ooi, Q. Gan, A polydimethylsiloxane-coated metal structure for all-day radiative cooling, Nat. Sustain. 2 (2019) 718–724.
[15] D. Chae, S. Son, Y. Liu, H. Lim, H. Lee, High-performance daytime radiative cooler and near-ideal selective emitter enabled by transparent sapphire substrate, Adv. Sci. (weinh.). 7 (2020) 2001577.
[16] N.N. Shi, C.-C. Tsai, F. Camino, G.D. Bernard, N. Yu, R. Wehner, Thermal physiology. keeping cool: enhanced optical reflection and radiative heat dissipation in saharan silver ants, Sci. 349 (2015) 298–301.
[17] S.-Y. Heo, G.J. Lee, D.H. Kim, Y.J. Kim, S. Ishii, M.S. Kim, T.J. Seok, B.J. Lee, H. Lee, Y.M. Song, A Janus emitter for passive heat release from enclosures, Sci. Adv. 6 (2020) eabb1906.
[18] K. Tang, K. Dong, J. Li, M.P. Gordon, F.G. Reichertz, H. Kim, Y. Rho, Q. Wang, C.-Y. Lin, C.P. Grigoropoulos, A. Javey, J.J. Urban, J. Yao, R. Levinson, J. Wu, Temperature-adaptive radiative coating for all-season household thermal regulation, Sci. 374 (2021) 1504–1509.
[19] Y. Peng, J. Chen, A.Y. Song, P.B. Catrysse, P.-C. Hsu, L. Cai, B. Liu, Y. Zhu, G. Zhou, D.S. Wu, H.R. Lee, S. Fan, Y. Cui, Nanoporous polyethylene microfibres for large-scale radiative cooling fabric, Nat. Sustain. 1 (2018) 105–112.
[20] D. Li, X. Liu, W. Li, Z. Lin, B. Zhu, Z. Li, J. Li, B. Li, S. Fan, J. Xie, J. Zhu, Scalable and hierarchically designed polymer film as a selective thermal emitter for high-performance all-day radiative cooling, Nat. Nanotechnol. 16 (2021) 153–158.
[21] T. Wang, Y. Wu, L. Shi, X. Hu, M. Chen, L. Wu, A structural polymer for highly efficient all-day passive radiative cooling, Nat. Commun. 12 (2021) 365.
[22] C. Cai, F. Chen, Z. Wei, C. Ding, Y. Chen, Y. Wang, Y. Fu, Large scalable, anti-ultraviolet, strong cellulose film with well-defined dual-pores for longtime daytime radiative cooling, Chem. Eng. J. 476 (2023) 146668.
[23] C. Cai, Y. Sun, Y. Chen, Z. Wei, Y. Wang, F. Chen, W. Cai, J. Ji, Y. Ji, Y. Fu, Large scalable, ultrathin and self-cleaning cellulose aerogel film for daytime radiative cooling, J. Bioresour. Bioprod. 8 (2023) 421–429.
[24] Y. Zhai, Y. Ma, S.N. David, D. Zhao, R. Lou, G. Tan, R. Yang, X. Yin, Scalable-manufactured randomized glass-polymer hybrid metamaterial for daytime radiative cooling, Science 355 (2017) 1062–1066.

[25] H. Zhang, K.C.S. Ly, X. Liu, Z. Chen, M. Yan, Z. Wu, X. Wang, Y. Zheng, H. Zhou, T. Fan, Biologically inspired flexible photonic films for efficient passive radiative cooling, PNAS 117 (2020) 14657–14666.
[26] J. Song, W. Zhang, Z. Sun, M. Pan, F. Tian, X. Li, M. Ye, X. Deng, Durable radiative cooling against environmental aging, Nat. Commun. 13 (2022) 4805.
[27] X. Wang, X. Liu, Z. Li, H. Zhang, Z. Yang, H. Zhou, T. Fan, Scalable flexible hybrid membranes with photonic structures for daytime radiative cooling, Adv. Funct. Mater. 30 (2020) 1907562.
[28] S. Jeon, S. Son, S.Y. Lee, D. Chae, J.H. Bae, H. Lee, S.J. Oh, Multifunctional daytime radiative cooling devices with simultaneous light-emitting and radiative cooling functional layers, ACS Appl. Mater. Interfaces 12 (2020) 54763–54772.
[29] X. Cai, L. Gao, J. Wang, D. Li, MOF-integrated hierarchical composite fiber for efficient daytime radiative cooling and antibacterial protective textiles, ACS Appl. Mater. Interfaces 15 (2023) 8537–8545.
[30] F.S. Hussain, N. Memon, Z. Khatri, Facile process for the development of antiviral cotton fabrics with nano-embossed copper oxide, ACS Omega 8 (2023) 18617–18625.
[31] M. Hosseini, A.W.H. Chin, M.D. Williams, S. Behzadinasab, J.O. Falkinham 3rd, L. L.M. Poon, W.A. Ducker, Transparent anti-SARS-CoV-2 and antibacterial silver oxide coatings, ACS Appl. Mater. Interfaces 14 (2022) 8718–8727.
[32] A.B. Younis, Y. Haddad, L. Kosaristanova, K. Smerkova, Titanium dioxide nanoparticles: recent progress in antimicrobial applications, Wiley Interdiscip. Rev. Nanomed. Nanobiotechnol. 15 (2023) e1860.
[33] P. Merkl, S. Long, G.M. McInerney, G.A. Sotiriou, Antiviral activity of silver, copper oxide and zinc oxide nanoparticle coatings against SARS-CoV-2, Nanomaterials (basel). 11 (2021) 1312.
[34] Y.H. Leung, A.M.C. Ng, X. Xu, Z. Shen, L.A. Gethings, M.T. Wong, C.M.N. Chan, M. Y. Guo, Y.H. Ng, A.B. Djurišić, P.K.H. Lee, W.K. Chan, L.H. Yu, D.L. Phillips, A.P. Y. Ma, F.C.C. Leung, Mechanisms of antibacterial activity of MgO: non-ROS mediated toxicity of MgO nanoparticles towards escherichia coli, Small 10 (2014) 1171–1183.
[35] Y. He, S. Ingudam, S. Reed, A. Gehring, T.P. Strobaugh Jr, P. Irwin, Study on the mechanism of antibacterial action of magnesium oxide nanoparticles against foodborne pathogens, J. Nanobiotechnology. 14 (2016) 54.
[36] Y.Y. Liao, A. Strayer-Scherer, J.C. White, R. De La Torre-Roche, L. Ritchie, J. Colee, G.E. Vallad, J. Freeman, J.B. Jones, M.L. Paret, Particle-size dependent bactericidal activity of magnesium oxide against Xanthomonas perforans and bacterial spot of tomato, Sci. Rep. 9 (2019) 18530.
[37] A. S, H.P. Kavitha, Magnesium oxide nanoparticles: effective antilarvicidal and antibacterial agents, ACS, Omega 8 (2023) 5225–5233.
[38] X. Yu, J. Chan, C. Chen, Review of radiative cooling materials: performance evaluation and design approaches, Nano Energy 88 (2021) 106259.
[39] M.-C. Huang, M. Yang, X.-J. Guo, C.-H. Xue, H.-D. Wang, C.-Q. Ma, Z. Bai, X. Zhou, Z. Wang, B.-Y. Liu, Y.-G. Wu, C.-W. Qiu, C. Hou, G. Tao, Scalable multifunctional radiative cooling materials, Prog. Mater Sci. 137 (2023) 101144.
[40] M. Hemath, S. Mavinkere Rangappa, V. Kushvaha, H.N. Dhakal, S. Siengchin, A comprehensive review on mechanical, electromagnetic radiation shielding, and thermal conductivity of fibers/inorganic fillers reinforced hybrid polymer composites, Polym. Compos. (2020) 3940–3965.
[41] W.B. Han, G.-J. Ko, S.M. Yang, H. Kang, J.H. Lee, J.-W. Shin, T.-M. Jang, S. Han, D.-J. Kim, J.H. Lim, K. Rajaram, A.J. Bandodkar, S.-W. Hwang, Micropatterned elastomeric composites for encapsulation of transient electronics, ACS Nano 17 (2023) 14822–14830.
[42] Y. Ji, Y. Sun, J. Muhammad, X. Li, Z. Liu, P. Tu, Y. Wang, Z. Cai, B. Xu, Fabrication of hydrophobic multilayered fabric for passive daytime radiative cooling, Macromol. Mater. Eng. 307 (2022) 2100795.
[43] W.B. Han, J.H. Lee, J.-W. Shin, S.-W. Hwang, Advanced materials and systems for biodegradable, transient electronics, Adv. Mater. 32 (2020) e2002211.
[44] W.B. Han, G.-J. Ko, K.-G. Lee, D. Kim, J.H. Lee, S.M. Yang, D.-J. Kim, J.-W. Shin, T.-M. Jang, S. Han, H. Zhou, H. Kang, J.H. Lim, K. Rajaram, H. Cheng, Y.-D. Park, S. H. Kim, S.-W. Hwang, Ultra-stretchable and biodegradable elastomers for soft, transient electronics, Nat. Commun. 14 (2023) 2263.
[45] H. Kang, W.B. Han, S.M. Yang, G.-J. Ko, Y. Ryu, J.H. Lee, J.-W. Shin, T.-M. Jang, K. Rajaram, S. Han, D.-J. Kim, J.H. Lim, C.-H. Eom, A.J. Bandodkar, S.-W. Hwang, Stretchable and biodegradable triboelectric nanogenerator based on elastomeric nanocomposites, Chem. Eng. J. 475 (2023) 146208.
[46] J. Feng, K. Gao, M. Santamouris, K.W. Shah, G. Ranzi, Dynamic impact of climate on the performance of daytime radiative cooling materials, Sol. Energy Mater. Sol. Cells 208 (2020) 110426.
[47] J. Huang, C. Lin, Y. Li, B. Huang, Effects of humidity, aerosol, and cloud on subambient radiative cooling, Int. J. Heat Mass Transf. 186 (2022) 122438.
[48] S.I. Jeong, B.-S. Kim, S.W. Kang, J.H. Kwon, Y.M. Lee, S.H. Kim, Y.H. Kim, In vivo biocompatibilty and degradation behavior of elastic poly(l-lactide-co-ε-caprolactone) scaffolds, Biomater. 25 (2004) 5939–5946.
[49] M. Demirel, Mechanical properties and cell viability of MgO-reinforced biografts fabricated for biomedical applications, Acta Bioeng. Biomech. 20 (2018) 83–90.
[50] A. Khalid, R. Norello, A.N. Abraham, J.-P. Tetienne, T.J. Karle, E.W.C. Lui, K. Xia, P.A. Tran, A.J. O'Connor, B.G. Mann, R. Boer, Y. He, A.M.C. Ng, A.B. Djurisic, R. Shukia, S. Tomlijenovic-Hanic, Biocompatible and biodegradable magnesium oxide nanoparticles with in vitro photostable near-infrared emission: short-term fluorescent markers, Nanomater. 9 (2019) 1360.